

Journal Pre-proofs

Zoledronate repositioning as a potential trypanocidal drug. *Trypanosoma cruzi* HPRT an alternative target to be considered

W.M. Valsecchi, J.M. Delfino, J. Santos, S.H. Fernández Villamil

PII: S0006-2952(21)00120-9
DOI: <https://doi.org/10.1016/j.bcp.2021.114524>
Reference: BCP 114524

To appear in: *Biochemical Pharmacology*

Received Date: 21 December 2020
Revised Date: 10 March 2021
Accepted Date: 11 March 2021

Please cite this article as: W.M. Valsecchi, J.M. Delfino, J. Santos, S.H. Fernández Villamil, Zoledronate repositioning as a potential trypanocidal drug. *Trypanosoma cruzi* HPRT an alternative target to be considered, *Biochemical Pharmacology* (2021), doi: <https://doi.org/10.1016/j.bcp.2021.114524>

This is a PDF file of an article that has undergone enhancements after acceptance, such as the addition of a cover page and metadata, and formatting for readability, but it is not yet the definitive version of record. This version will undergo additional copyediting, typesetting and review before it is published in its final form, but we are providing this version to give early visibility of the article. Please note that, during the production process, errors may be discovered which could affect the content, and all legal disclaimers that apply to the journal pertain.

© 2021 Published by Elsevier Inc.



1 **Zoledronate repositioning as a potential trypanocidal drug.**

2 ***Trypanosoma cruzi* HPRT an alternative target to be considered.**

3 **WM. Valsecchi^{a,b,1}, JM. Delfino^{a,b}, J. Santos^{a,b,2}, SH. Fernández Villamil^{a,c,1}**

4 *a* Departamento de Química Biológica, Facultad de Farmacia y Bioquímica, Universidad de Buenos Aires
5 (UBA).

6 *b* Instituto de Química y Físicoquímica Biológicas (IQUIFIB-CONICET).

7 *c* Instituto de Investigaciones en Ingeniería Genética y Biología Molecular (INGEBI-CONICET).

8
9 Running Head: Zoledronate repositioned against *T. cruzi*.

10
11 *I* Address correspondence to Silvia H. Fernández Villamil: silvia.villamil@gmail.com,
12 s.villamil@ingebi.conicet.gov.ar, Vuelta de Obligado 2490 (1428), Ciudad Autónoma de Buenos Aires,
13 Argentina, Phone (5411) 4783 2871, FAX (5411)4786-8578; and Wanda M. Valsecchi: wvalsecchi@gmail.com,
14 wvalsecchi@qb.ffyb.uba.ar Junín 956 (1113), Ciudad Autónoma de Buenos Aires, Argentina, Phone
15 (5411) 5287-4110.

16 *2* Present address Javier Santos: Instituto de Biociencias, Biotecnología y Biología Traslacional (iB3).
17 Departamento de Fisiología y Biología Molecular y Celular, Facultad de Ciencias Exactas y Naturales, UBA.

18

19 **ABSTRACT**

20 Chagas disease is caused by the protozoan parasite *Trypanosoma cruzi* and affects
21 7 million people worldwide. Considering the side effects and drug resistance shown by
22 current treatments, the development of new anti-Chagas therapies is an urgent need. *T. cruzi*
23 hypoxanthine phosphoribosyltransferase (TcHPRT), the key enzyme of the purine salvage
24 pathway, is essential for the survival of trypanosomatids. Previously, we assessed the
25 inhibitory effect of different bisphosphonates (BPs), HPRT substrate analogues, on the
26 activity of the isolated enzyme. BPs are used as a treatment for bone diseases and growth
27 inhibition studies on *T. cruzi* have associated BPs action with the farnesyl diphosphate
28 synthase inhibition. Here, we demonstrated significant growth inhibition of epimastigotes in
29 the presence of BPs and a strong correlation with our previous results on the isolated
30 TcHPRT, suggesting this enzyme as a possible and important target for these drugs. We also
31 found that the parasites exhibited a delay of S phase in the presence of zoledronate pointing
32 out enzymes involved in the cell cycle, such as TcHPRT, as intracellular targets. Moreover,
33 we validated that micromolar concentrations of zoledronate are capable to interfere with the
34 progression of cell infection by this parasite. Altogether, our findings allow us to propose the
35 repositioning of zoledronate as a promising candidate against Chagas disease and TcHPRT as
36 a new target for future rational design of antiparasitic drugs.

37

38 **Keywords:** hypoxanthine phosphoribosyltransferase (HPRT), *Trypanosoma cruzi*, growth
39 inhibition, bisphosphonates, zoledronate.

40 **Abbreviations:** *Trypanosoma cruzi* hypoxanthine phosphoribosyltransferase (TcHPRT),
41 human HPRT (HsHPRT), Bisphosphonate (BP).

42 1. INTRODUCTION

43 Chagas disease is a neglected disease caused by the protozoan parasite
44 *Trypanosoma cruzi* that affects approximately 7 million people worldwide, mainly in endemic
45 areas of 21 continental Latin American countries (WHO)
46 (<https://www.who.int/chagas/epidemiology/en/>), although cases have also been reported in
47 non-endemic areas. Currently, approved treatments for Chagas disease are based on
48 nifurtimox and benznidazole (BZN), available since 1965 and 1971, respectively. Both drugs
49 show a high variability in the efficacy, nifurtimox has been demonstrated to cause adverse
50 effects in long-term therapies, while BZN has been related to toxicity and drug resistance [1-
51 3]. Therefore, the development of more effective and better-tolerated new anti-Chagas drugs
52 is an urgent need.

53 Nucleotide synthesis in parasitic protozoa only occurs by the recovery pathway which
54 requires a key enzyme called hypoxanthine phosphoribosyltransferase (HPRT) [4] (Figure 1).
55 Considering that *T. cruzi* has no alternative pathways for GMP and IMP production than the
56 salvage route, it is expected that inhibitors of TcHPRT should prevent its growth by blocking
57 the synthesis of their DNA/RNA, a strategy previously used for the development of
58 chemotherapeutics that prevent the growth and proliferation of parasites [5]. HPRT activity
59 was reported as essential for *Leishmania donovani*, *Plasmodium falciparum*, *T. cruzi* and
60 *Mycobacterium tuberculosis* [6-9]. Given these facts, *T. cruzi* HPRT (TcHPRT) has been
61 proposed as a prime target for drugs aimed at treating parasitic diseases (*see TDRtargets*
62 *Database*, <http://tdrtargets.org>).

63 Regarding the design of inhibitory molecules that show selectivity for TcHPRT, an
64 approach is to design molecules with high mimicry to the transition state of the reaction
65 catalyzed [10]. With the aim of testing molecules similar in structure to PRPP, we previously
66 carried out the study of the effect produced on TcHPRT activity of a set of bisphosphonates

67 (BPs), molecules that emulate the pyrophosphate moiety of PRPP [11, 12]. In the past, several
68 BPs have been established as therapeutic agents for the prevention of skeletal complications
69 connected with multiple myeloma or bone metastases [13]. It was also demonstrated that BPs
70 reduce the risk of fractures and increase bone mineral density so that they are widely used for
71 the treatment of menopausal osteoporosis in women, osteoporosis induced by glucocorticoids,
72 and imperfect osteogenesis in children [14, 15]. Currently, the BP named zoledronate has
73 been matter under study in principal areas of medical science such as breast cancer [16, 17]
74 and bone marrow lesions [18, 19].

75 Bisphosphonates accumulate in the *T. cruzi* acidocalcisomes and can inhibit enzymes
76 involved in inorganic and organic pyrophosphate reactions such as farnesyl pyrophosphate
77 synthase (FPPS), nevertheless other potential target molecules have not been discarded [3].
78 Here, we examine the effect of a select group of BPs on *T. cruzi* growth and postulate
79 TcHPRT as a possible target for these drugs.

80 Drug repositioning involves finding novel indications for approved drugs, giving new
81 answers to old problems; using drugs already established for human use greatly shortens
82 development timeframes saving time and money, since these compounds have shown proven
83 toxicological and pharmacokinetic profiles, and the evaluation phases have already been
84 approved. In this regard, we advance the argument of repositioning zoledronate as a candidate
85 drug against Chagas disease.

86 2. MATERIALS AND METHODS

87 2.1. Culture media and reagents

88 *T. cruzi* epimastigotes were cultured in LIT (Liver Infusion Tryptose): (5 g L⁻¹ liver
89 infusion, 5 g L⁻¹ bacto-tryptose, 68 mM NaCl, 5.3 mM KCl, 22 mM Na₂HPO₄, 0.2 % (W/V)
90 glucose, and 0.002 % (W/V) hemin) supplemented with 10 % fetal bovine serum (FBS),
91 100 U mL⁻¹ penicillin and 100 µg mL⁻¹ streptomycin) for 7 days at 28 °C. FBS was from

92 Natocor, Argentina. Bacto-tryptose and liver infusion were from Difco Laboratories, Detroit,
93 MI. Vero cells were cultured in MEM (Sigma-Aldrich) supplemented with
94 2 mM L-glutamine, 100 U mL⁻¹ penicillin, 100 µg mL⁻¹ streptomycin and 3 % FBS, at 37 °C
95 and 5 % CO₂ atmosphere. The set of BPs used in this work was provided by GADOR S.A.,
96 Buenos Aires. Other reagents were from Sigma-Aldrich, St. Louis, MO, USA.

97 2.2. Screening of inhibitors

98 *T. cruzi* epimastigote *Tulahuen strain* was grown at 28 °C in LIT medium supplemented
99 with 10 % FBS, 100 µg mL⁻¹ streptomycin and 100 U mL⁻¹ penicillin for 4 days (exponential
100 growth). Parasites (10⁶ mL⁻¹, 100 µl) were placed in 96-well sterile plates in the presence of
101 the corresponding BP solution. Control samples were grown in LIT in the absence of BP.
102 Optical density (OD_{600 nm}) of the cultures was determined for 4 days to follow cell viability.
103 All conditions were assayed in triplicates in each of 14 experiences. The significance of the
104 results was analyzed using the Bonferroni test. IC₅₀ values were obtained by non-linear
105 regression logistic functions, using GraphPad Prism 6.1 for Windows. Results are shown as
106 mean ± standard deviation (SD).

107 TcHPRT activity was determined in a previous work [11], showing a biphasic behavior
108 in the presence of BPs. Two hyperbola equations were fitted to the experimental data by a
109 nonlinear regression procedure using *OriginPro 2017* to obtain the K_{0.5} values. Results are
110 expressed as mean ± SD.

111 2.3. Cell cycle analysis on epimastigotes cultured in the presence of zoledronate

112 *T. cruzi* epimastigotes were cultured in LIT medium with or without
113 1.5 mM zoledronate. After 4 days of growth, cells were fixed with 70 % ethanol, stained with
114 propidium iodide (Sigma-Aldrich, St. Louis, MO, US) and then analyzed by flow cytometry.

115 **2.4. Hydroxyurea-induced synchronization and flow cytometry analysis**

116 *T. cruzi* epimastigotes in exponential growth were diluted in LIT medium up to
117 $2 \times 10^6 \text{ mL}^{-1}$ to be synchronized at G1 phase with 20 mM hydroxyurea (Sigma-Aldrich, St.
118 Louis, MO, US) for 18 h. Synchronized epimastigotes were washed 3 times with cold PBS
119 and resuspended in LIT medium supplemented with or without 0.8 mM zoledronate. Both
120 cultures were incubated at 28 °C and 1 mL samples were collected every 2 h during 24 h. Cell
121 cycle was analyzed by flow cytometry using propidium iodide and the samples previously
122 fixed with 70 % cold ethanol.

123 Data analysis was made with FlowJo X10 software. Briefly, after a 10000-events
124 collection, cells with the expected size and complexity were selected to make the histogram.
125 Phases G1, S and G2/M were defined over the histogram generated and those settings were
126 fixed all over the analysis. Finally, control and treatment histograms were superimposed and
127 the percentage of epimastigotes in each phase was calculated. It is worth noting that the
128 experiment was made by triplicate with similar results.

129 **2.5. β -galactosidase assay**

130 The assay was performed on Vero cells (ATCC® CCL-81™) in a p96 plate. Cells,
131 (10^4 seeded per well) were infected in MOI (multiplicity of infection) 10:1 with
132 trypomastigotes carrying the gene for β -galactosidase [20]. After 24 h incubation period, fresh
133 media plus each study drug was added to infected monolayers. At 96 h p.i. (post-infection),
134 cell culture media was removed and Tulahuen β -galactosidase parasites were lysed in 100 μL
135 lysis buffer (25 mM Tris-HCl, pH 7.8; 2 mM EDTA; 1 % Triton X100; 10 % glycerol; 2 mM
136 DTT), a condition in which cells were incubated for 15 min at 37 °C. Then, 100 μL of
137 reaction buffer (200 mM $\text{NaH}_2\text{PO}_4/\text{Na}_2\text{HPO}_4$, pH 7.0; 2 mM MgCl_2 ; 100 μM
138 β -mercaptoethanol; 1.33 mg mL^{-1} o-nitrophenyl- β -D-galactopyranoside (ONPG)) was added
139 and the absorbance increase, as a consequence of ONPG hydrolysis, was detected at 420 nm

140 in a Synergy HTX multi-mode microplate reader during the following 30, 45, and 60 min. All
141 conditions were assayed in triplicates of five independent experiences. IC50 values were
142 obtained by non-linear regression logistic functions, using GraphPad Prism 6.1. Results are
143 expressed as mean \pm SD. All reagents were from (Sigma-Aldrich, St. Louis, MO, US).

144 **2.6. Alamar blue assay**

145 The test was performed on Vero cells in a p96 plate. Cells (10^4 per well) were seeded in
146 MEM (100 μ L) supplemented with 10 % FBS. Cells were incubated for 24 h and the media
147 was replaced by MEM-3 % FBS with the study drugs. Cells were incubated in this condition
148 for 72 h at 37 °C and 5 % CO₂ atmosphere. Then, the medium was replaced by fresh medium
149 and resazurin (Sigma-Aldrich, St. Louis, MO, US) solution (10 μ g mL⁻¹ final concentration).
150 Resazurin shows an increased fluorescence in its reduced form. After 30 min fluorescence
151 was measured (excitation at 530 nm and emission at 590 nm).

152 **3. RESULTS**

153 **3.1. *In vitro* trypanocidal activity of BPs**

154 Previously we reported that BP derivatives alendronate, ibandronate, lidadronate,
155 olpadronate, pamidronate, and zoledronate, show inhibitory effect on the recombinant
156 TcHPRT [11]. These BPs display a characteristic biphasic behavior on enzymatic activity,
157 showing activation at low concentrations whereas behaving as inhibitors at high
158 concentrations. Considering that ibandronate had turned out to be the best inhibitor and
159 olpadronate, the best activator, we tested both on the human variant HsHPRT. At a
160 concentration as high as 500 μ M, both ibandronate and olpadronate scarcely inhibit HsHPRT
161 (21.2 and 4.1 % respectively) as compared to the control sample. This result opens the
162 possibility of considering these and related BPs as trypanocidal agents. In this regard, we
163 evaluated the response of epimastigotes to BPs and analyzed the culture growth rate relative
164 to the control up to day 4 of growth. Concentrations were selected as multiples of the IC50 for

165 purified recombinant TcHPRT. All concentrations assayed inhibited cell growth, an effect that
166 becomes significant since day 2 (Figure 2). Zoledronate and ibandronate proved to be the best
167 inhibitors. Nevertheless, statistical analysis showed no significant differences for 1.5 mM
168 zoledronate between days 1 and 4, which indicates that cell growth is totally arrested after
169 24 h exposure to the drug. The same analysis in the case of ibandronate shows that the growth
170 is inhibited since day 3 at the same concentration, suggesting a relatively greater potency for
171 zoledronate than ibandronate. At similar concentrations, the other BPs assayed show much
172 reduced ability to inhibit the growth of epimastigotes, with olpadronate and pamidronate
173 showing an intermediate effect (reaching a plateau at about 50 %). Both alendronate and
174 lidadronate showed only roughly 20 % of growth inhibition under similar conditions
175 (~1.2 mM).

176 We calculated the BP concentrations required to inhibit 50 % of TcHPRT activity on
177 the purified protein ($K_{0.5}$) and to inhibit 50 % of parasite growth at day 4 (IC₅₀). The
178 inhibitory potency in each case was (zoledronate/ibandronate) >> (pamidronate/olpadronate)
179 > (lidadronate/alendronate) (Table 1). This outcome suggests a correlation in the inhibitory
180 effect seen on TcHPRT and the epimastigotes growth inhibition. Moreover, these results also
181 suggest that these BPs are efficiently incorporated into parasites, which is important when
182 considering the multiplicity of factors that would arbitrate their transport.

183 **3.2. BPs affect *T. cruzi* proliferation and cell infection**

184 To further study the effect of BPs on the intracellular replicative form amastigote, we
185 seeded Vero cells on 96-well plates and β -galactosidase-expressing trypomastigotes were
186 allowed to remain in contact with cells for 24 h. After that period, medium was removed and
187 replaced with fresh medium added with the corresponding inhibitors. Parasite counts were
188 then determined spectrophotometrically by measuring the product of the enzymatic reaction
189 96 h p.i. A graphical representation of the infection schedule is shown in Figure 3. The

190 compounds were tested at different concentrations ranging from 0–2.5 mM. It should be noted
191 that in the experimental design, we excluded pamidronate and olpadronate, since these are the
192 BPs showing intermediate effects both on epimastigotes and on the isolated enzyme. The
193 result for each condition is expressed relative to the value obtained for the infection in the
194 absence of inhibitors. In order to test the possible toxicity of these compounds on host cells,
195 we evaluated the viability of the Vero cells by using the Alamar Blue method. Zoledronate,
196 ibandronate and alendronate led to a decrease in the measured β -galactosidase activity,
197 indicating a decrease in the infection levels (Figure 3). These results also indicate that BPs
198 manage to cross the membrane of Vero cells, and efficiently reach their target molecules.
199 While the same concentration of zoledronate and alendronate (50 μ M) causes a similar
200 decrease in the infection level (~85 %), alendronate is too toxic for the host cell (~75 %
201 toxicity). By contrast, lidadronate is not toxic to Vero cells, albeit it is also well tolerated by
202 parasites in the same range of concentrations.

203 Thereafter, we estimated the selectivity index (SI), a metric that relates the IC₅₀ for
204 Vero cells, with the IC₅₀ for the amastigotes (Table 2), thus BPs with higher SI will be
205 considered the best inhibitors. As we had previously interpreted, these results showed
206 antiparasitic potencies in the following order: zoledronate > ibandronate > alendronate >
207 lidadronate. At similar low μ M IC₅₀ values, the SI for zoledronate (55.5) compares with
208 advantage to that corresponding to BZN (20.1) [21], the most widely used drug for the
209 treatment of Chagas disease, placing the former as an interesting drug candidate.

210 **3.3. Zoledronate impairs epimastigote cell cycle**

211 As *T. cruzi* has no alternative pathways to bypass HPRT for purine nucleotides
212 production, it is expected that inhibitors of TcHPRT should block the synthesis of
213 DNA/RNA, impairing the cell cycle. With the aim of studying whether the cell cycle is
214 arrested at a particular phase, we cultured *T. cruzi* epimastigotes for 4 days in the absence or

215 in the presence of 1.5 mM of zoledronate, and we determined then the populations in each cell
216 cycle phase by flow cytometry (Figure 4). Results showed alterations in the pattern observed
217 when parasites were grown in the presence of zoledronate (Figure 4C). It is possible that this
218 difference lies in the difficulty for parasites to complete the cell cycle in the presence of this
219 BP.

220 Considering these observations, we challenged a previously synchronized culture using
221 hydroxyurea (HU) —an inhibitor of DNA synthesis— allowing next the parasites to complete
222 their cycle in the absence or in the presence of zoledronate. We choose to test 0.8 mM of drug
223 since this concentration was the lowest exhibiting the maximum inhibitory effect at day 4 of
224 growth. While non-synchronized cells show their population distributed in similar proportions
225 among the three phases of the cycle, we found that synchronized epimastigotes are mainly at
226 G1/S boundary, the valley of the S region is very marked and there are very few cells in the
227 G2/M phase. Besides, control epimastigote cell cycle was completed in 18-20 h, in agreement
228 with previous reports [22]. Results depicted as histograms in Figure 5A show that both
229 cultures untreated and treated with 0.8 mM zoledronate progressed similarly through G1.
230 However, it is possible to observe a delay in the cell cycle starting at 6h after HU removal,
231 indicating that the S phase proceeds more slowly in treated cells. The observed lag is
232 accentuated as time goes by, and therefore cells exposed to zoledronate require more time to
233 return to the G1 phase. Note that between 14 and 18 h after HU removal most control cells
234 culminate the S phase, while in the culture exposed to zoledronate still 20 % of cells remain in
235 this phase decreasing only after 22 h (Figure 5C). This delay explains why at 22 h post HU
236 removal, twice this population of cells does not complete mitosis, as compared to control cells
237 (39.6 % cells in G2/M for zoledronate vs. 19.9 % for control) (Figure 5B and D).

238 All in all, these observations indicate the difficulty in the progression through the cell
239 cycle of the culture exposed to the drug and suggest an effect of zoledronate on enzymes

240 related to the cell cycle. Accordingly, it is possible to consider TcHPRT among the targets of
241 this BP.

242 4. DISCUSSION

243 Many efforts to identify new targets for Chagas disease are constantly pursued, as
244 recently reviewed [23, 24]. However, since nifurtimox and BZN were discovered no other
245 drug was introduced into the market and they are efficient only in the acute phase [1].
246 Regarding the development of efficient and well-tolerated drugs against the parasite,
247 repositioning of drugs used for other pathologies is cost-effective and a strategy
248 recommended by the World Health Organization (WHO) to tackle neglected diseases like
249 Chagas.

250 BPs have been available for the treatment of osteoporosis, Paget's disease, the
251 hypercalcemia of malignancy, and bone metastases derived from various cancer types. We
252 reported that BPs inhibit TcHPRT, an essential enzyme for *T. cruzi* and rationalized the
253 structural principles underlying the inhibitory effects observed by each BP by docking
254 *in silico* [11]. The BPs studied here show inhibitory effect on the proliferation of the parasite,
255 revealing zoledronate the higher relative potency. This result agrees with our previous
256 statement on the inhibitory effects on TcHPRT of these BPs, where we suggested that the
257 higher inhibitory power of zoledronate could be due to the presence of a diffuse positive
258 charge in the aromatic ring of imidazole, a feature resembling the transition state of the
259 pyrophosphorolysis and condensation reactions [11]. Further co-crystallization assays of
260 TcHPRT and other HPRTs with BPs might shed light on the differences in the mechanism of
261 action of zoledronate in those enzymes.

262 Looking for inhibitory compounds that mimic substrates or products of key enzymes for
263 parasite survival, molecules acting on several target enzymes could be interesting candidates,
264 since compensating for their absence would be more difficult for the cell. On this matter, it

265 has been described that TcFPPS is inhibited by BPs [25, 26], and Demoro *et al.* stated that the
266 tested compounds produce a decrease in the proliferation of *T. cruzi* amastigotes as a
267 consequence of a multi-target effect [27]. Such multi-target action, probably involves
268 TcHPRT, an option that has not been considered so far.

269 Zoledronate (one of the two compounds with greater inhibitory power on recombinant
270 TcHPRT) was the best growth inhibitor for both the epimastigote and amastigote forms of the
271 parasite. To shed light on the intracellular mechanism of action of zoledronate, we studied its
272 effect on epimastigotes cell cycle. Since TcHPRT is essential for purine nucleotides
273 production, it is expected that inhibitors of TcHPRT block the parasite DNA/RNA synthesis.
274 Our results indicate that zoledronate makes difficult the transit through the S phase of the cell
275 cycle, which could suppose an action on enzymes related to DNA synthesis such as TcHPRT.
276 The correlation between our results on the recombinant TcHPRT and the replicative forms of
277 the parasite strongly suggests that the enzyme pointed out could be one of the most important
278 targets.

279 Among other BPs, zoledronate has also been tested as a potential agent against
280 *Leishmania tarentolae* [28], *Trypanosoma brucei* [29], *Plasmodium falciparum* and
281 *Entamoeba histolytica* [30], and lipophilic analogs of zoledronate and risedronate were
282 postulated as potent antimalarial drugs [31]. A double-hit strategy combining inhibitors of
283 host and parasite pathways was proposed as a novel approach against toxoplasmosis by using
284 zoledronic acid and atorvastatin [32]. These results support zoledronate as a promising
285 antiprotozoal candidate.

286 Recently, a meta-analysis suggests that alendronate and zoledronate are the BPs of
287 choice for the treatment of osteoporosis [33], and zoledronate is the most extensively used BP
288 in cancer therapy for preventing skeletal complications in patients with bone metastases. New
289 formulations of alendronate or zoledronate by encapsulation in liposomes or nanoparticles are

290 being investigated to increase their effectiveness and reduce the doses used [34]. On the other
291 hand, intravenous administration of zoledronate [35] and the combination of zoledronate with
292 other drugs [36, 37] are being tested in order to reduce its adverse effects. These studies can
293 be inspiring for stimulating research on the treatment of other diseases.

294 An open-label pharmacokinetic and pharmacodynamic study of zoledronic acid
295 performed in patients who received 4 mg dose displays plasmatic concentrations of
296 approximately 320 ng mL⁻¹ [38]. These serum levels are in the same order as zoledronate
297 IC₅₀ for the intracellular form of the parasite. Moreover, we determined SI values for
298 zoledronate > 50, agreeing with the highest inhibitory effect on the parasite and low
299 cytotoxicity observed. This is particularly significant since a SI of > 50 is considered adequate
300 for trypanocidal drugs, which reinforce the repurposing of zoledronate as a possible
301 anti-Chagas agent [39-41]. Regarding the drug repositioning strategy, nowadays the combined
302 therapy of drugs with different mechanisms of action is also considered an adequate strategy
303 for achieving a synergistic effect and delaying or overcoming the appearance of drug
304 resistance [27, 42, 43]. Likewise, the combination of BZN with new drugs is also an
305 alternative under study [21, 44, 45].

306 To sum up, for its essential role TcHPRT has been suggested as a potential target
307 against *T. cruzi*. Our results show that the inhibition of TcHPRT effectively affects the
308 parasite cell cycle, leading to a decrease in parasite growth and impairment in the progression
309 of cell infection. Zoledronate, a BP with therapeutic uses in constant updating, appears as a
310 promising candidate for drug repurposing as an anti-Chagas drug due to its effects on
311 TcHPRT, although this argument does not rule out the involvement of other molecular
312 targets. These results encourage the scientific community to further investigate zoledronate to
313 facilitate their use for the treatment of this trypanosomiasis and other neglected diseases.

314 **ACKNOWLEDGMENTS**

315 We thank Dra. Miriam Dziubecki and Dr. Emilio Roldán from GADOR SA, Buenos
316 Aires for providing the set of BPs used in this work. We also thank Rodrigo G. Ducati, PhD
317 (Albert Einstein College of Medicine, USA), for gently providing us with HsHPRT,
318 William A. Agudelo (Fundación Instituto de Inmunología de Colombia (FIDIC),
319 Bogotá D.C., Colombia), for his comments and suggestions, and
320 Salomé C. Vilchez Larrea, PhD (INGEBI, Argentina) for her collaboration in cell culture and
321 β -galactosidase-trypanomastigotes production. This work was supported by Agencia Nacional
322 de Promoción Científica y Tecnológica PICT 2015-0898 and Universidad de Buenos Aires.

323 **CREDIT AUTHOR STATEMENT**

324 **Wanda M. Valsecchi:** Conceptualization; Methodology; Validation; Formal analysis;
325 Investigation; Writing - Original Draft; Writing - Review & Editing; Visualization.
326 **José María Delfino:** Conceptualization; Writing - Review & Editing; Visualization.
327 **Javier Santos:** Conceptualization; Writing - Review & Editing; Visualization.
328 **Silvia H. Fernández Villamil:** Conceptualization; Methodology; Validation; Formal
329 analysis; Investigation; Resources; Writing - Original Draft; Writing - Review & Editing;
330 Visualization; Supervision; Project administration; Funding acquisition.

331 **COMPETING INTERESTS**

332 The authors declare no competing interests.

333 **REFERENCES**

- 334 [1] T.O. Custodio-Leite, Developments on treatment of Chagas disease– from discovery to current times,
335 European Review for Medical and Pharmacological Sciences 23 (2019) 11.
336 [2] R. Martín-Escolano, J. Martín-Escolano, R. Ballesteros-Garrido, N. Cirauqui, B. Abarca, M.J. Rosales, M.
337 Sánchez-Moreno, R. Ballesteros, C. Marín, Repositioning of leishmanicidal [1,2,3]Triazololo[1,5-a]pyridinium
338 salts for Chagas disease treatment: *Trypanosoma cruzi* cell death involving mitochondrial membrane
339 depolarisation and Fe-SOD inhibition, Protozoology Research (2020).
340 [3] J.A. Urbina, Specific chemotherapy of Chagas disease: Relevance, current limitations and new approaches,
341 Acta Tropica 115 (2010) 55-68.

- 342 [4] R.L. Berens, J.J. Marr, S.W. LaFon, D.J. Nelson, Purine Metabolism in *Trypanosoma cruzi*, Molecular and
343 Biochemical Parasitology 3 (1981) 187-196.
- 344 [5] D.T. Keough, D. Rejman, R. Pohl, E. Zborníková, D. Hockova, T. Croll, M.D. Edstein, G.W. Birrell, M.
345 Chavchich, L.M.J. Naesens, G.K. Pierens, I.M. Brereton, L.W. Guddat, The Design of *Plasmodium vivax*
346 Hypoxanthine-Guanine Phosphoribosyltransferase Inhibitors as Potential Antimalarial Therapeutics, ACS
347 Chemical Biology 13(1) (2018) 9.
- 348 [6] J.M. Boitz, B. Ullman, A Conditional Mutant Deficient in Hypoxanthine-guanine Phosphoribosyltransferase
349 and Xanthine Phosphoribosyltransferase Validates the Purine Salvage Pathway of *Leishmania donovani*, The
350 Journal of Biological Chemistry 281(23) (2006) 16084-90.
- 351 [7] P.A. Dawson, D.A.E. Cochran, B.T. Emmerson, R.B. Gordon, Inhibition of *Plasmodium falciparum*
352 hypoxanthine-guanine phosphoribosyltransferase mRNA by antisense oligodeoxynucleotide sequence,
353 Molecular and Biochemical Parasitology 60 (1993) 153-156.
- 354 [8] D.M. Freymann, M.A. Wenck, J.C. Engel, J. Feng, P.J. Focia, A.E. Eakin, S.P. Craig III, Efficient
355 identification of inhibitors targeting the closed active site conformation of the HPRT from *Trypanosoma cruzi*,
356 Chemistry and Biology 7 (2000) 957-69.
- 357 [9] J. Le Nours, E.M.M. Bulloch, Z. Zhang, D.R. Greenwood, M.J. Middleditch, J.M.J. Dickson, E.N. Baker,
358 Structural Analyses of a Purine Biosynthetic Enzyme from *Mycobacterium tuberculosis* Reveal a Novel Bound
359 Nucleotide, The Journal of Biological Chemistry 286(47) (2011) 40706-40716.
- 360 [10] C.M. Li, P.C. Tyler, R.H. Furneaux, G. Kicska, Y. Xu, C. Grubmeyer, M.E. Girvin, V.L. Schramm,
361 Transition-state analogs as inhibitors of human and malarial hypoxanthine-guanine phosphoribosyltransferases,
362 nature structural biology 6(6) (1999) 6.
- 363 [11] W.M. Valsecchi, A. Cousido-Siah, L.A. Defelipe, A. Mitschler, A. Podjamy, J. Santos, J.M. Delfino, The
364 role of the C-terminal region on the oligomeric state and enzymatic activity of *Trypanosoma cruzi* hypoxanthine
365 phosphoribosyl transferase, Biochimica et Biophysica Acta 1864 (2016) 655-666.
- 366 [12] D. Fernández, M.A. Wenck, S.P. Craig III, J.M. Delfino, The purine transferase from *Trypanosoma cruzi* as
367 a potential target for bisphosphonate-based chemotherapeutic compounds, Bioorganic & Medicinal Chemistry
368 Letters 14 (2004) 4501-4.
- 369 [13] R.G.G. Russell, N.B. Watts, F.H. Ebetino, M.J. Rogers, Mechanisms of action of bisphosphonates:
370 similarities and differences and their potential influence on clinical efficacy, Osteoporos Int 19 (2008) 733-759.
- 371 [14] U.A. Liberman, S.R. Weiss, J. Bröll, H.W. Minne, H. Quan, N.H. Bell, J. Rodriguez-Portales, R.W.D. Jr., J.
372 Dequeker, M. Favus, Effect of oral alendronate on bone mineral density and the incidence of fractures in
373 postmenopausal osteoporosis. The Alendronate Phase III Osteoporosis Treatment Study Group., The New
374 England Journal of Medicine 333(22) (1995) 7.
- 375 [15] M. McClung, S.T. Harris, P.D. Miller, D.C. Bauer, S. Davison, L. Dian, D.A. Hanley, D.L. Kendler, C.K.
376 Yuen, E.M. Lewiecki, Bisphosphonate Therapy for Osteoporosis: Benefits, Risks, and Drug Holiday, The
377 American Journal of Medicine 126(1) (2013) 8.
- 378 [16] J.R. Gralow, W.E. Barlow, A.H.G. Paterson, J.L. Miao, D.L. Lew, A.T. Stopeck, D.F. Hayes, D.L.
379 Hershman, M.M. Schubert, M. Clemons, C.H.V. Poznak, E.C. Dees, J.N. Ingle, C.I. Falkson, A.D. Elias, M.J.
380 Messino, J.H. Margolis, S.R. Dakhil, H.K. Chew, K.Z. Dammann, J.S. Abrams, R.B. Livingston, G.N.
381 Hortobagyi, Phase III Randomized Trial of Bisphosphonates as Adjuvant Therapy in Breast Cancer: S0307, J
382 Natl Cancer Inst 112(7) (2020) 36.
- 383 [17] H. Sözel, F. Yılmaz, Symptomatic hypocalcemia following a single dose of zoledronic acid in a patient with
384 bone metastases secondary to breast cancer, Journal of Oncology Pharmacy Practice 0(0) (2020) 4.
- 385 [18] F. Müller, K.A. Appelt, C. Meier, N. Suhm, Zoledronic acid is more efficient than ibandronic acid in the
386 treatment of symptomatic bone marrow lesions of the knee, Knee Surgery, Sports Traumatology, Arthroscopy 28
387 (2020) 10.
- 388 [19] G. Cai, D. Aitken, L.L. Laslett, J.-P. Pelletier, J. Martel-Pelletier, C. Hill, L. March, A.E. Wluka, Y. Wang,
389 B. Antony, L. Blizzard, T. Winzenberg, F. Cicuttini, G. Jones, Effect of Intravenous Zoledronic Acid on
390 Tibiofemoral Cartilage Volume Among Patients With Knee Osteoarthritis With Bone Marrow Lesions: A
391 Randomized Clinical Trial, JAMA 323(15) (2020) 11.
- 392 [20] F. Buckner, C. Verlinde, A. Flammé, W. Voorhis, Efficient Technique for Screening Drugs for Activity
393 against *Trypanosoma cruzi* using parasites expressing β -galactosidase, Microbiology 40 (1996) 6.
- 394 [21] V. Puente, A. Demaria, F.M. Frank, A. Battle, M.E. Lombardo, Anti-parasitic effect of vitamin C alone and
395 in combination with benznidazole against *Trypanosoma cruzi*, PloS Neglected Tropical Diseases 12(9) (2018)
396 13.
- 397 [22] M. Potenza, S. Schenkman, M. Laverrière, M.T. Tellez-Iñón, Functional characterization of TcCYC2 cyclin
398 from *Trypanosoma cruzi*, Experimental Parasitology 132 (2012) 537-545.
- 399 [23] M.R. Miranda, M.M. Sayé, Chagas Disease Treatment: From New Therapeutic Targets to Drug Discovery
400 and Repositioning, Editorial Current Medicinal Chemistry 26(36) (2019) 2.

- 401 [24] S.S. Santos, R.V.d. Araújo, J. Giarolla, O.E. Seoud, E.I. Ferreira, Searching drugs for Chagas disease,
402 leishmaniasis and schistosomiasis: a brief review, *International Journal of Antimicrobial Agents* 55(4) (2020).
- 403 [25] L.R. Garzoni, A. Caldera, M.d.N.L. Meirelles, S.L. de Castro, R. Docampo, G.A. Meints, E. Oldfield, J.A.
404 Urbina, Selective in vitro effects of the farnesyl pyrophosphate synthase inhibitor risnedronate on *Trypanosoma*
405 *cruzi*, *International Journal of Antimicrobial Agents* 23 (2004) 273-285.
- 406 [26] S.H. Szajnman, A. Montalvetti, Y. Wang, R. Docampo, J.B. Rodriguez, Bisphosphonates derived from fatty
407 acids are potent inhibitors of *Trypanosoma cruzi* farnesyl pyrophosphate synthase, *Bioorg Med Chem Lett*
408 13(19) (2003) 3231-5.
- 409 [27] B. Demoro, S. Rostán, M. Moncada, Z.-H. Li, R. Docampo, C.O. Azar, J.D. Maya, J. Torres, D. Gambino,
410 L. Otero, Ibandronate metal complexes: solution behavior and antiparasitic activity, *Journal of Biological*
411 *Inorganic Chemistry* 23 (2018) 10.
- 412 [28] A.T. Christensen, C.C. McLauchlan, A. Dolbecq, P. Mialane, M.A. Jones, Studies of the Effectiveness of
413 Bisphosphonate and Vanadium-Bisphosphonate Compounds *In Vitro* against Asexual *Leishmania tarentolae*,
414 *Oxidative Medicine and Cellular Longevity* 2016 (2016) 12.
- 415 [29] G. Yang, W. Zhu, K. Kim, S.Y. Byun, G. Choi, K. Wang, J.S. Cha, H.-S. Cho, E. Oldfield, J.H. No, *In*
416 *Vitro* and *In Vivo* Investigation of the Inhibition of *Trypanosoma brucei* Cell Growth by Lipophilic
417 Bisphosphonates, *Antimicrobial agents and chemotherapy* 59(12) (2015) 7530 –7539.
- 418 [30] S. Ghosh, J.M.W. Chan, C.R. Lea, G.A. Meints, J.C. Lewis, Z.S. Tovian, R.M. Flessner, T.C. Loftus, I.
419 Bruchhaus, H. Kendrick, S.L. Croft, R.G. Kemp, S. Kobayashi, T. Nozaki, E. Oldfield, Effects of
420 Bisphosphonates on the Growth of *Entamoeba histolytica* and *Plasmodium* Species *In Vitro* and *In Vivo*, *Journal*
421 *Med. Chem.* 47 (2004) 13.
- 422 [31] J.H. No, F.d.M. Dossin, Y. Zhang, Y.-L. Liua, W. Zhua, X. Feng, J.A. Yoo, E. Lee, K. Wang, R. Hui, L.H.
423 Freitas-Junior, E. Oldfield, Lipophilic analogs of zoledronate and risnedronate inhibit *Plasmodium geranylgeranyl*
424 *diphosphate synthase (GGPPS)* and exhibit potent antimalarial activity, *PNAS* 109(11) (2012) 6.
- 425 [32] Z.-H. Li, C. Li, S.H. Szajnman, J.B. Rodriguez, S.N.J. Morena, Synergistic Activity between Statins and
426 Bisphosphonates against Acute Experimental Toxoplasmosis, *Antimicrobial agents and chemotherapy* 61(8)
427 (2017) 10.
- 428 [33] S.G. Albert, S. Reddy, Clinical evaluation of cost efficacy of drugs for treatment of osteoporosis: a meta-
429 analysis, *Endocrine Practice* 27(7) (2017) 38.
- 430 [34] N.M. La-Beck, X. Liu, H. Shmeeda, C. Shudde, A.A. Gabizon, Repurposing amino-bisphosphonates by
431 liposome formulation for a new role in cancer treatment, *Seminars in Cancer Biology* Dec 23:S1044-
432 579X(19)30396-7. (2019).
- 433 [35] A. Grey, Intravenous zoledronate for osteoporosis: less might be more, *Therapeutic Advances in*
434 *Musculoskeletal Disease* 8(4) (2016) 5.
- 435 [36] P.M. Wiziack-Zago, I.M. Oliveira-Sousa, L. Servat-Medina, M. Pedroza-Jorge, L.G. Lima-Neto, V. Hass,
436 X. Li, A.L.T.G. Ruiz, D. Saxena, M.A. Foglio, Standardized *Arrabidaea chica* Extract Shows Cytoprotective
437 Effects in Zoledronic Acid-Treated Fibroblasts and Osteoblasts, *Clinical, Cosmetic and Investigational Dentistry*
438 12 (2020) 7.
- 439 [37] S. Zafar, D.E. Coates, M.P. Cullinan, B.K. Drummond, T. Milne, G.J. Seymour, Zoledronic acid and
440 geranylgeraniol regulate cellular behaviour and angiogenic gene expression in human gingival fibroblasts,
441 *Journal of Oral Pathology and Medicine* 43 (2014) 11.
- 442 [38] A. Skerjanec, J. Berenson, C. Hsu, P. Major, W.H.M. Jr., C. Ravera, H. Schran, J. Seaman, F. Waldmeier,
443 The Pharmacokinetics and Pharmacodynamics of Zoledronic Acid in Cancer Patients with Varying Degrees of
444 Renal Function, *Journal of Clinical Pharmacol* 43 (2003) 9.
- 445 [39] M.V. Papadopoulou, W.D. Bloomer, H.S. Rosenzweig, Ivan P. O'Shea, S.R. Wilkinson, M. Kaiser, Eric
446 Chatelain, J.-R. Ioset, Discovery of potent nitrotriazole-based antitrypanosomal agents: *In vitro* and *in vivo*
447 evaluation, *Bioorganic and Medicinal Chemistry* 23(19) (2015) 10.
- 448 [40] R. Paucar, E. Moreno-Viguri, S. Pérez-Silanes, Challenges in Chagas Disease Drug Discovery: A Review,
449 *Current Medicinal Chemistry* 23 (2016) 17.
- 450 [41] S. Nwaka, A. Hudson, Innovative lead discovery strategies for tropical diseases, *Nature Reviews Drug*
451 *Discovery* 5 (2006) 15.
- 452 [42] M.R. Simões-Silva, J.S.D. Araújo, R.B. Peres, P.B.D. Silva, M.M. Batista, L.D.D. Azevedo, M.M. Bastos,
453 M.T. Bahia, N. Boechat, M.N.C. Soeiro, Repurposing strategies for Chagas disease therapy: the effect of
454 imatinib and derivatives against *Trypanosoma cruzi*, *Parasitology* (2019) 7.
- 455 [43] R. Sánchez-Delgado, K. Lazard, L. Rincón, J. Urbina, Toward a novel metal-based chemotherapy against
456 tropical diseases. 1. Enhancement of the efficacy of clotrimazole against *Trypanosoma cruzi* by complexation to
457 ruthenium in RuCl₂(clotrimazole), *Journal Med. Chem.* 36(14) (1993) 4.
- 458 [44] I. Molina, J.G. Prat, F. Salvador, B. Treviño, E. Sulleiro, N. Serre, D. Pou, S. Roure, J. Cabezas, L. Valerio,
459 A. Blanco-Grau, A. Sánchez-Montalvá, X. Vidal, A. Pahissa, Randomized Trial of Posaconazole and
460 Benzimidazole for Chronic Chagas' Disease, *The new england journal of medicine* 370(20) (2014) 10.

461 [45] M. Sayé, L. Gauna, E. Valera-Vera, C. Reigada, M.R. Miranda, C.A. Pereira, Crystal violet structural
 462 analogues identified by *in silico* drug repositioning present anti-*Trypanosoma cruzi* activity through inhibition of
 463 proline transporter TcAAAP069, *PLoS Neglected Tropical Diseases* 14(1) (2020) 23.

464

465 FIGURE LEGENDS

466 **Figure 1. Purine recovery pathway.** HPRT catalyzes the transfer of ribose 1-phosphate from
 467 phosphoribosyl pyrophosphate (PRPP) to hypoxanthine (Hx) or guanine bases, yielding IMP or GMP,
 468 respectively, and pyrophosphate (PPi) (highlighted in red). Besides, HPRT can salvage guanine, and in some
 469 cases xanthine. APRT, adenine phosphoribosyltransferase, and XPRT, xanthine phosphoribosyltransferase.
 470 The *de novo* pathway (involving several enzymatic steps) to generate IMP from PRPP, carbon dioxide
 471 (CO₂), amino acids, and tetrahydrofolate derivatives (THF) is also indicated.

472 **Figure 2. Epimastigotes cultured in the presence of BPs for 96 h.** Each column represents the growth
 473 percentage ± SD. Bonferroni multiple analysis was used; in each group (*) p ≤ 0.0001, (+) p ≤ 0.001,
 474 (‡) p ≤ 0.01 and (#) p ≤ 0.05. The indicated statistical analyses were carried out for individual days, and
 475 referred to the control (black symbols) or to the highest concentration of each drug (red symbols).

476 **Figure 3. *T. cruzi* proliferation and cell infection.** The infection protocol scheme is shown on the top. The
 477 parasite count was estimated by absorbance at 420 nm according to the β-galactosidase activity protocol.
 478 Vero cells viability in each condition was estimated by Alamar blue assay. In all cases, data is presented as
 479 mean ± SD.

480 **Figure 4. Flow cytometry analysis of non-synchronized *T. cruzi* epimastigotes in the presence of
 481 zoledronate.** (A) Control epimastigotes sample; Ca and Cb are experimental duplicates. (B) Zoledronate
 482 exposed epimastigotes (1.5 mM); Za and Zb indicate experimental duplicates. (C) Ca and Za comparison.
 483 Population percentages are detailed in the insets.

484 **Figure 5. Cell cycle phases of epimastigotes cultured in the absence or in the presence of zoledronate.**
 485 Histograms belonging to control (red) and 0.8 mM zoledronate exposed (blue) cultures (A). To facilitate the
 486 comparison, population percentages corresponding to phase G1 (B), S (C), and G2/M (D) are shown at each
 487 time post HU-release.

488 CREDIT AUTHOR STATEMENT

489 **Wanda M. Valsecchi:** Conceptualization; Methodology; Validation; Formal analysis;
 490 Investigation; Writing - Original Draft; Writing - Review & Editing; Visualization. **José**
 491 **María Delfino:** Conceptualization; Writing - Review & Editing; Visualization. **Javier**
 492 **Santos:** Conceptualization; Writing - Review & Editing; Visualization. **Silvia H. Fernández**
 493 **Villamil:** Conceptualization; Methodology; Validation; Formal analysis; Investigation;
 494 Resources; Writing - Original Draft; Writing - Review & Editing; Visualization; Supervision;
 495 Project administration; Funding acquisition.

496

Table 1. Comparison between $K_{0.5}$ (TcHPRT) and IC50 (epimastigotes) values.

Bisphosphonate	$K_{0.5}$ (μM)	IC50 (μM)
Alendronate	>7000	>5000
Lidaronate	>7000	>5000
Pamidronate	197.8 \pm 13.4	2857 \pm 120
Olpadronate	193.1 \pm 24.3	1640 \pm 100
Zoledronate	162.3 \pm 23.2	60.5 \pm 10.1
Ibandronate	154.4 \pm 17.3	87.4 \pm 15.1

497

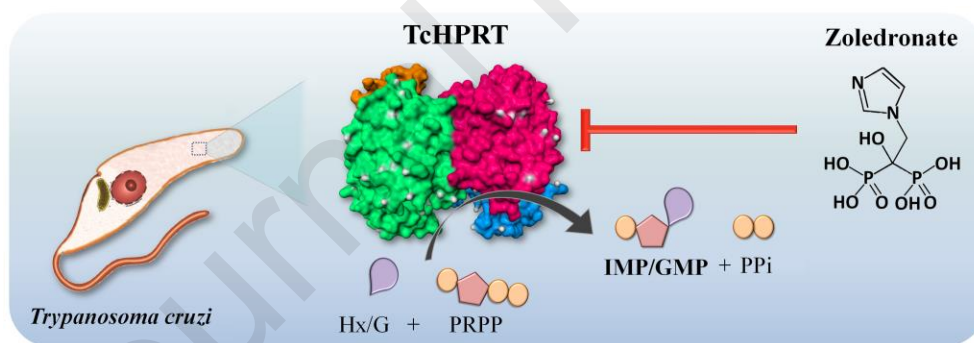
498

Table 2. IC 50 and Selectivity Index values for the selected compounds.

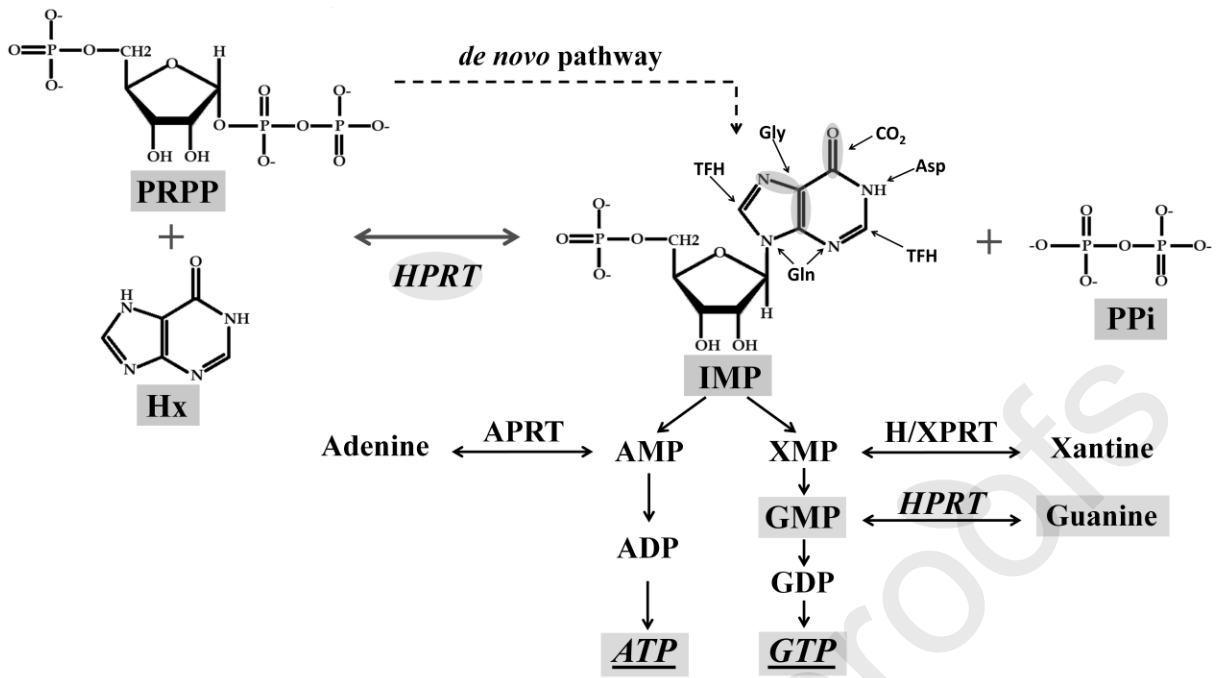
Compound	(IC50 μM)		SI
	Vero	<i>T. cruzi</i>	
BZN	82.8 \pm 2.8	4.1 \pm 0.4	20.1
Alendronate	18.9 \pm 2.6	6.6 \pm 0.2	2.8
Lidaronate	>2500	>2500	-
Zoledronate	322.2 \pm 37.8	5.8 \pm 0.3	55.5
Ibandronate	1199 \pm 232	105.4 \pm 15.6	11.4

499

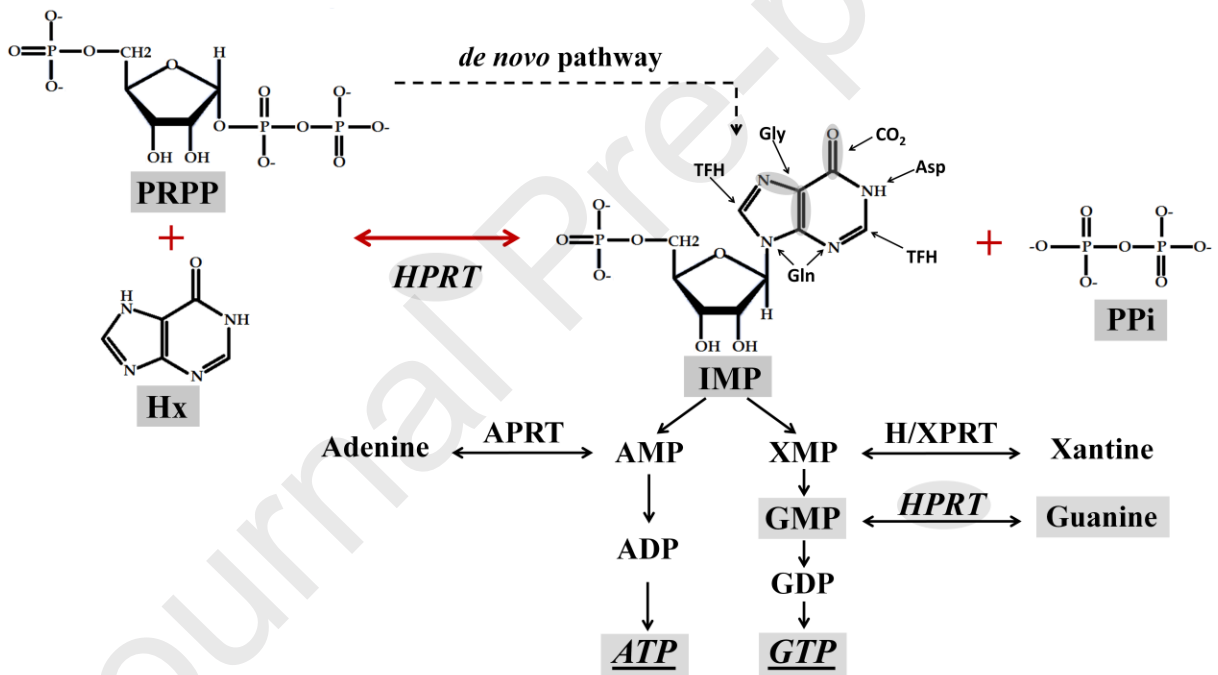
500



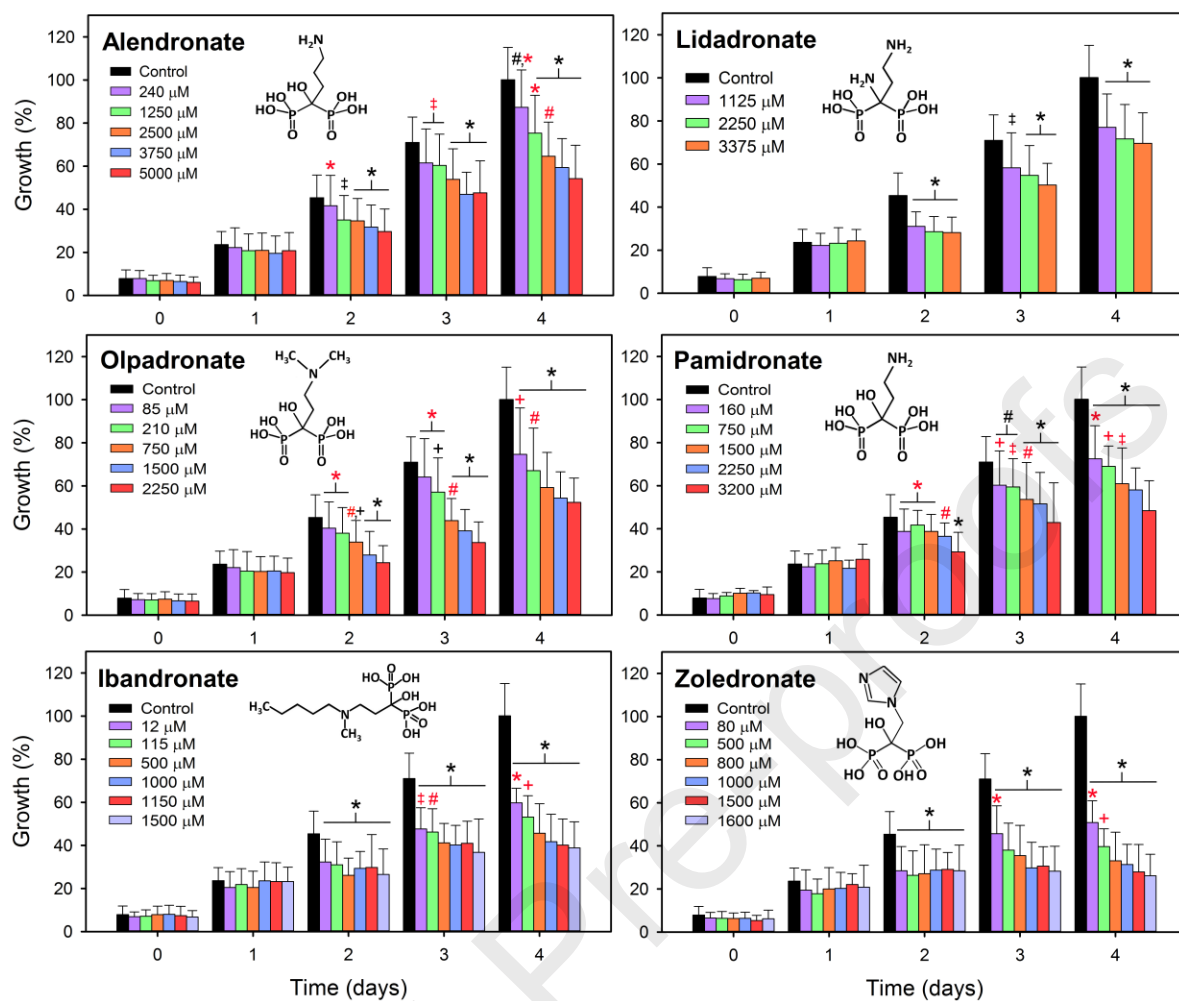
501



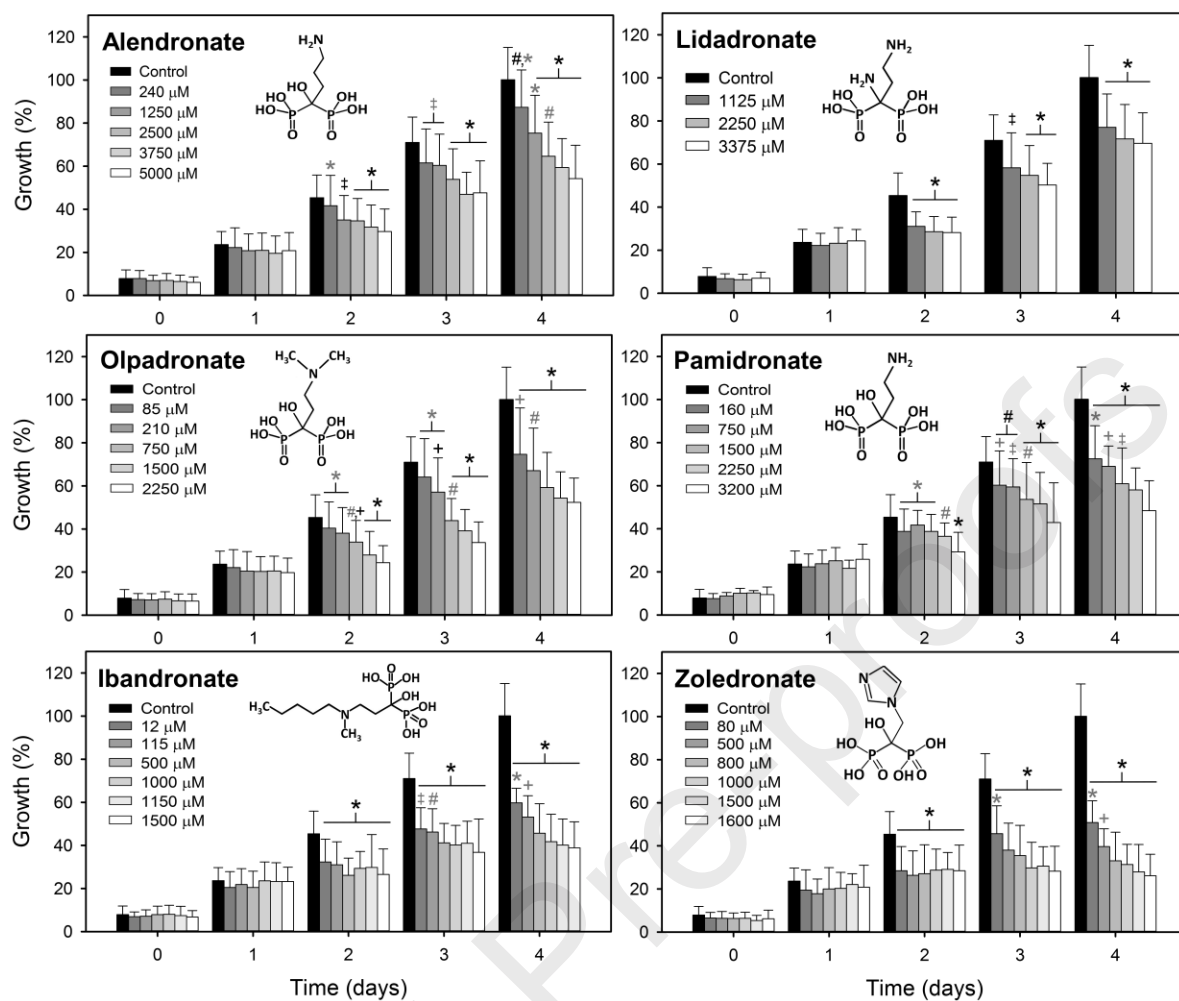
502



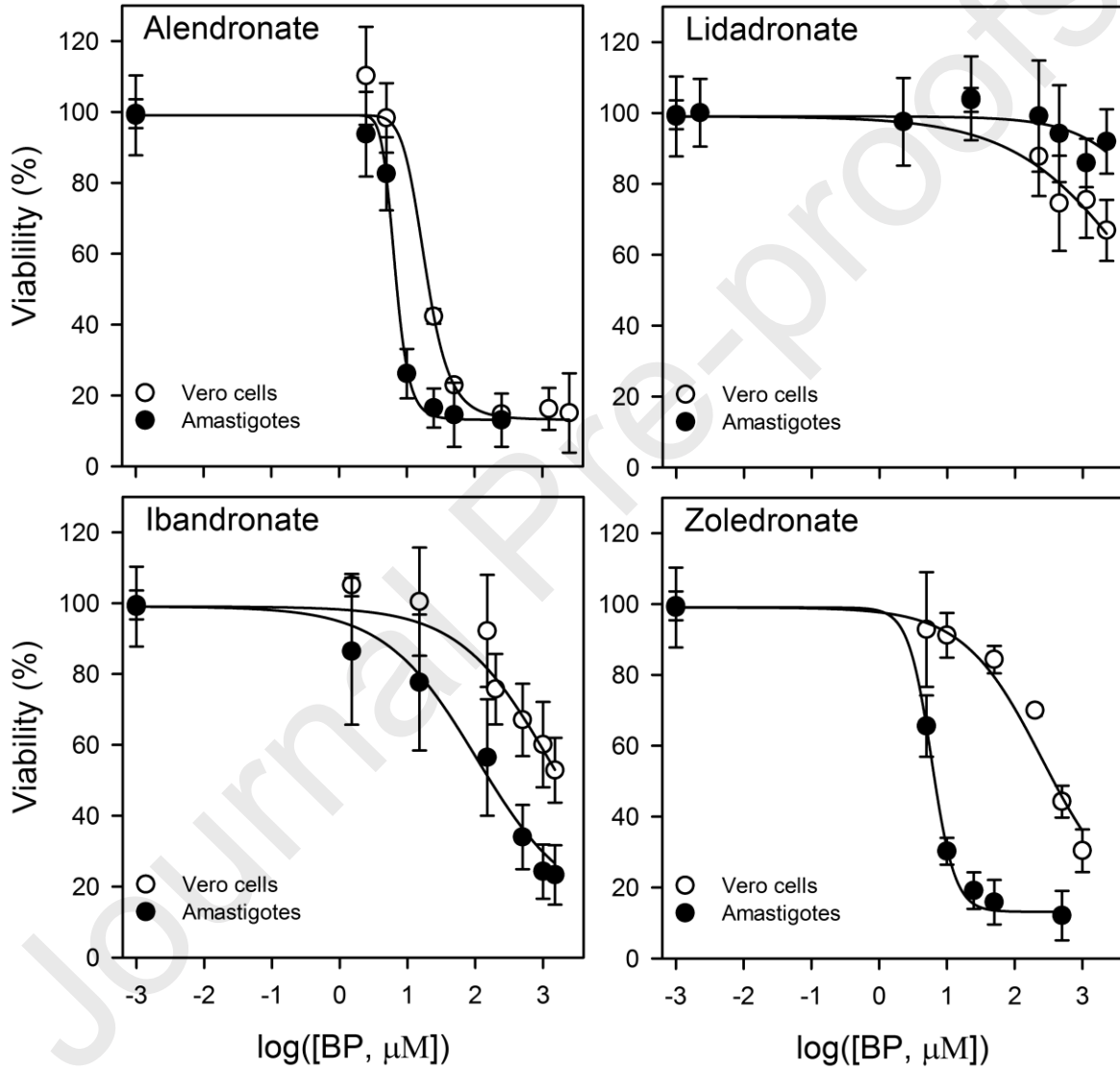
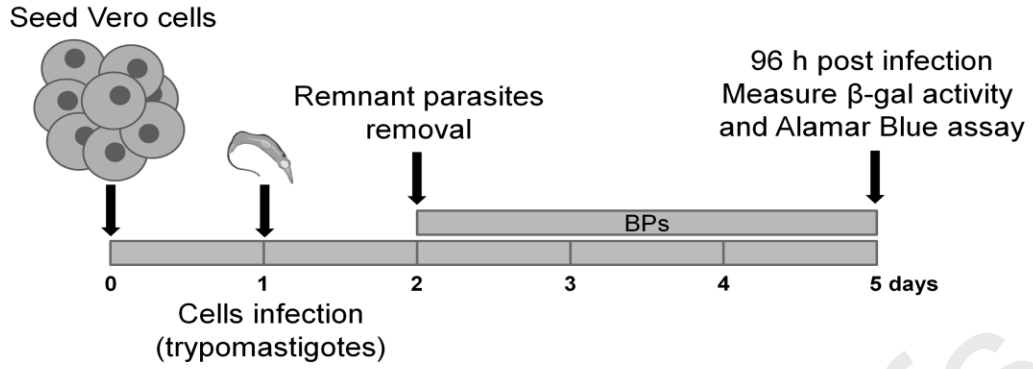
503



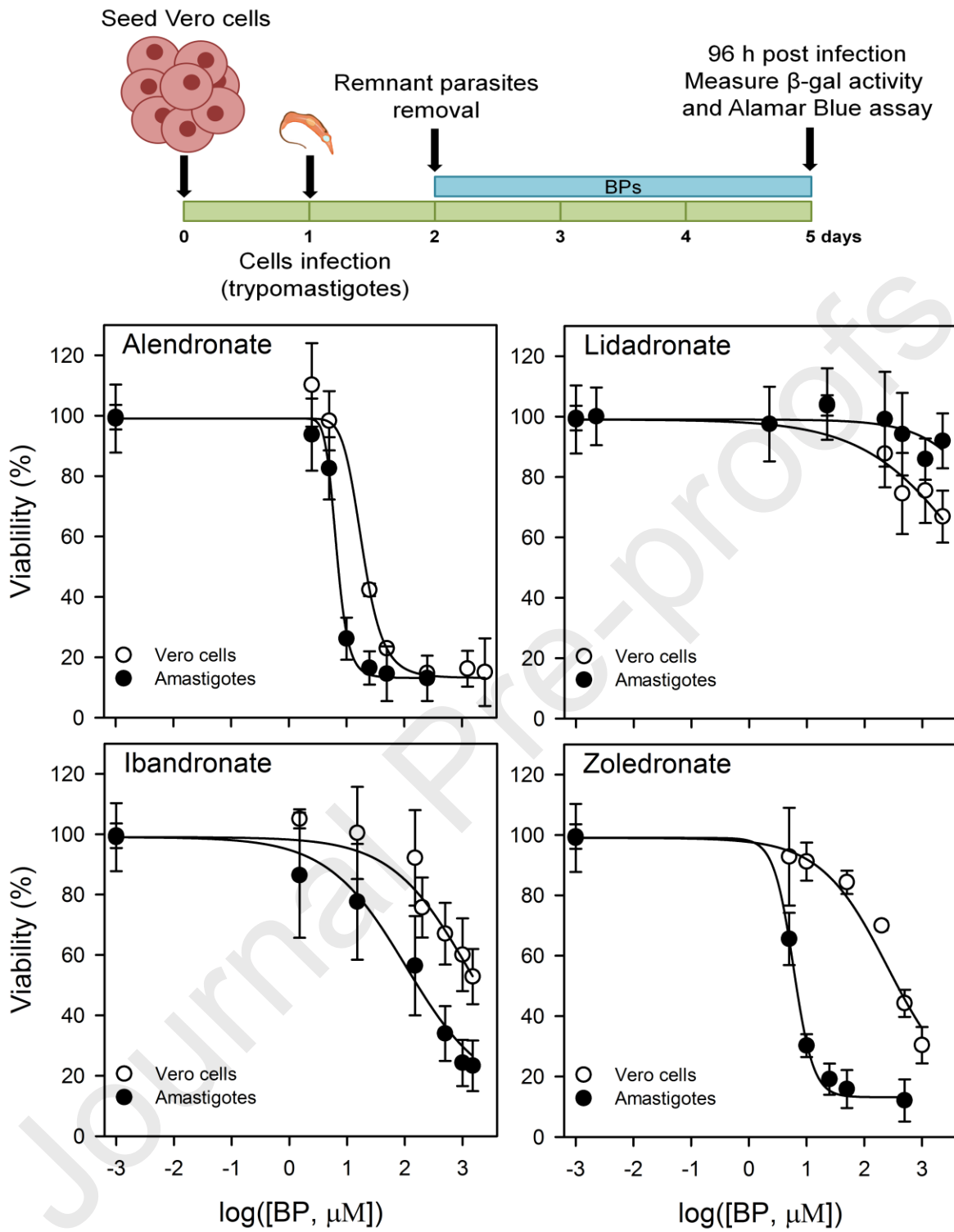
504



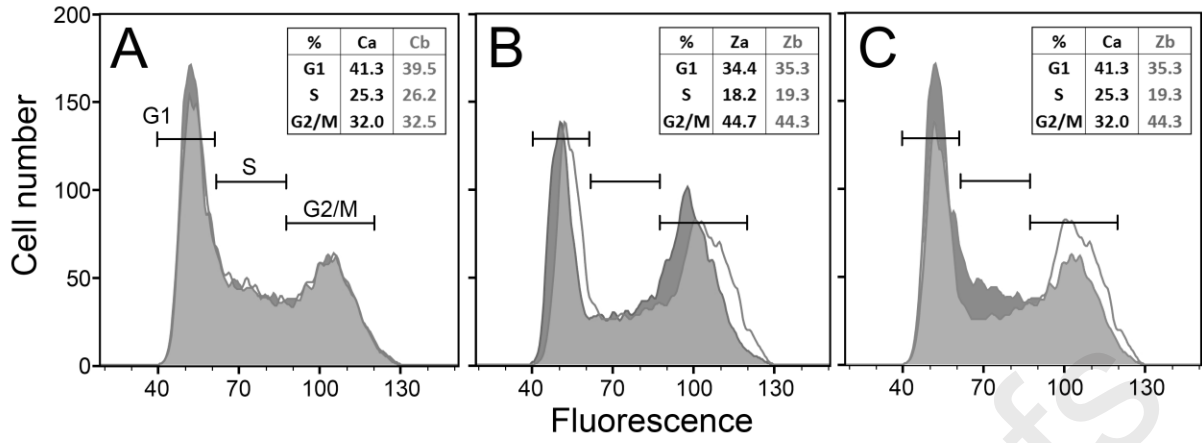
505



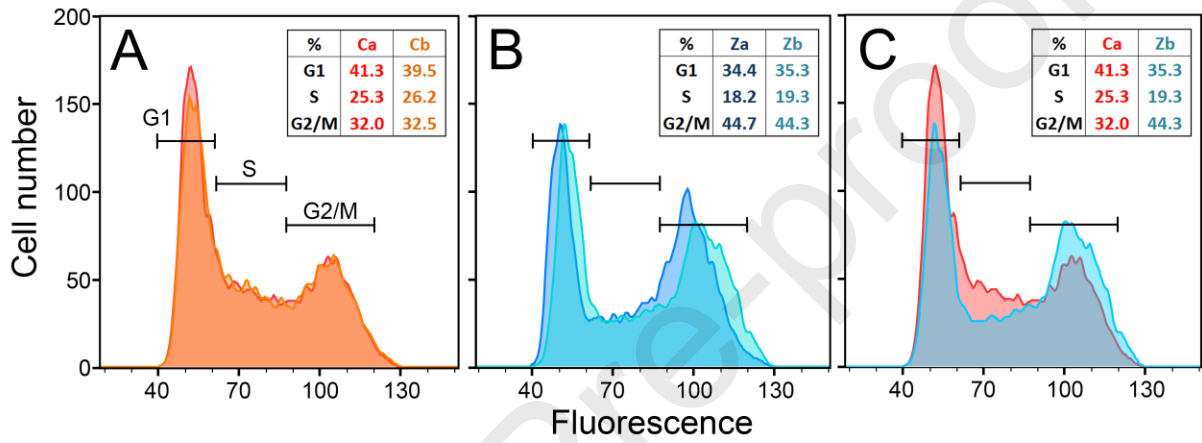
506



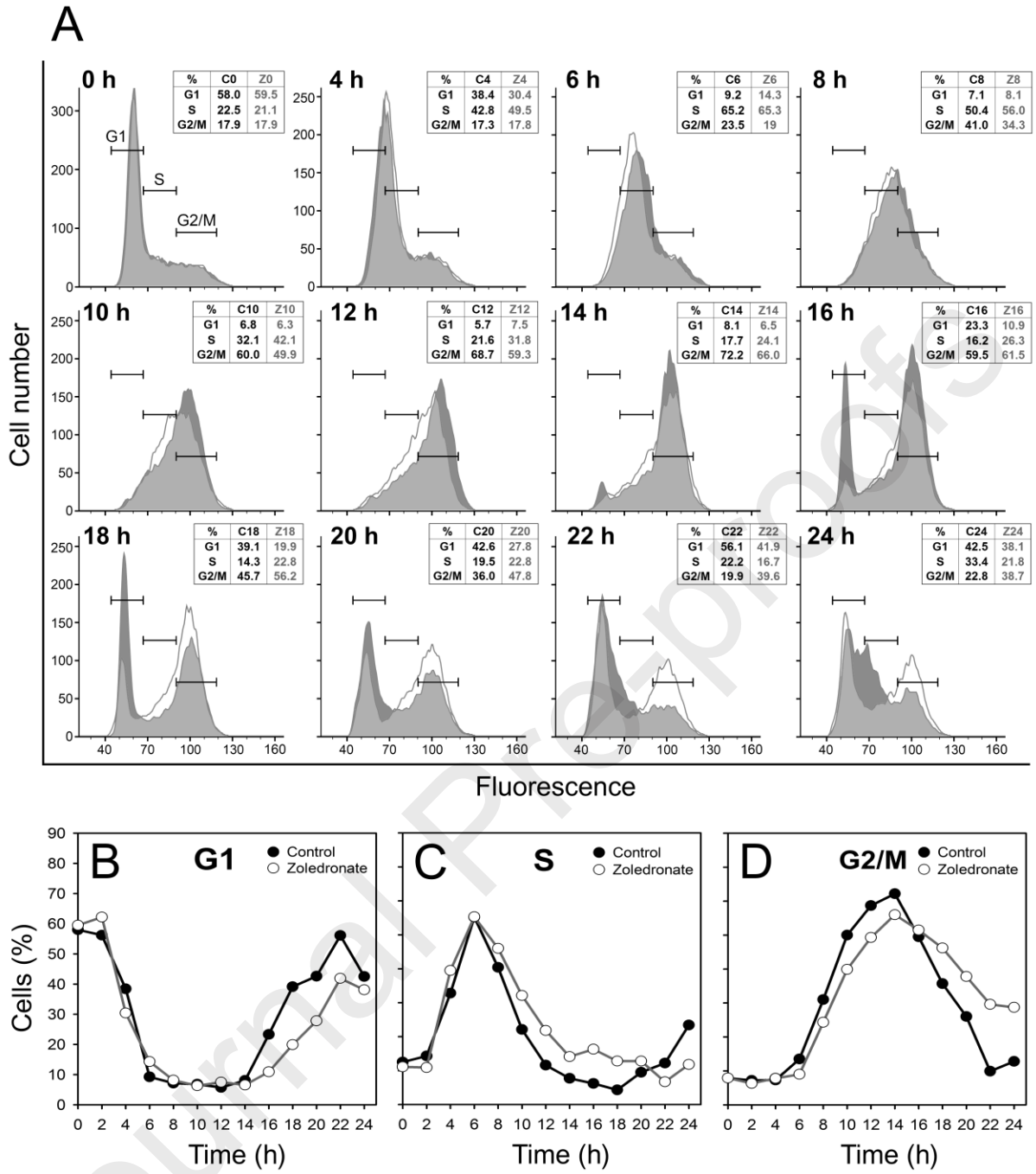
507



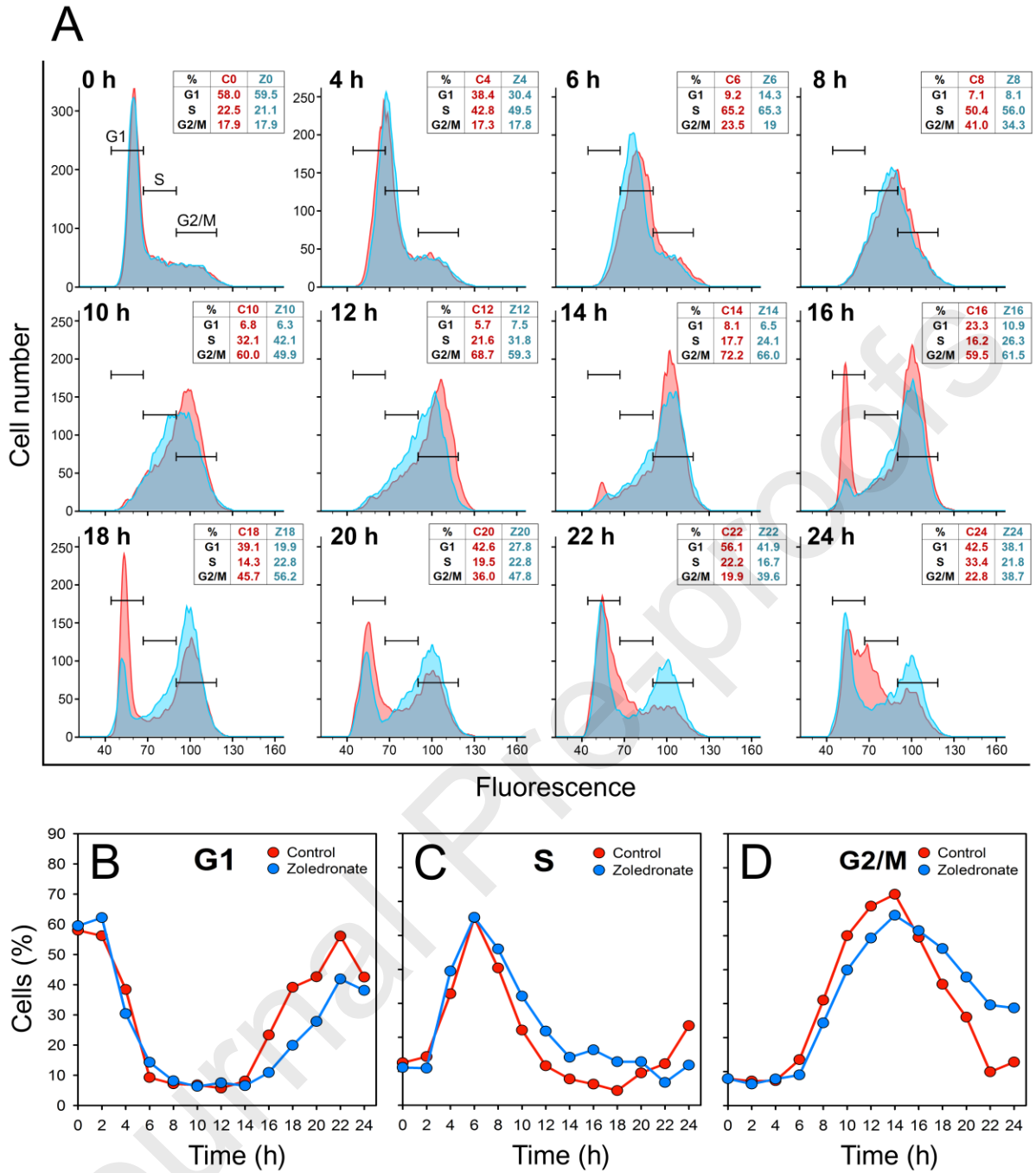
508



509



510



511